Dalton Transactions

RSCPublishing

ARTICLE

Nucleophilic Behaviour of Dioxo- and Thiooxophosphorane Complexes [MoCp(CO)$_2${*E,P*-EP(O)(2,4,6-C$_6$H$_2$^{t}Bu$_3$)}]$^-$ (E = O, S).†

Cite this: DOI: 10.1039/x0xx00000x

Received 00th ****** 2014,
Accepted 00th ****** 2014

DOI: 10.1039/x0xx00000x

www.rsc.org/

María Alonso, M. Angeles Alvarez, M. Esther García, Daniel García-Vivó,* and Miguel A. Ruiz*

The title anions were prepared as (DBU-H)$^+$ salts upon reaction of the oxophosphinidene complex (H-DBU)[MoCp(CO)$_2${P(O)R*}] with either dimethyldioxirane or elemental sulphur (R* = 2,4,6-C$_6$H$_2$^{t}Bu$_3$; Cp = η^5-C$_5$H$_5$, DBU = 1,8-diazabicyclo[5.4.0]undec-7-ene). The dioxophosphorane complex failed to react with MeI at room temperature, but reacted readily with (Me$_3$O)BF$_4$ to give the phosphonite complex [MoCp{*O,P*-OP(OMe)R*}(CO)$_2$]. In contrast, the thiooxophosphorane complex reacted with MeI to give the thiolophosphinide derivative [MoCp{*S,P*-(MeS)P(O)R*}(CO)$_2$], whereas its reaction with (Me$_3$O)BF$_4$ gave a mixture of the latter complex and the phosphonothiolate isomer [MoCp{*S,P*-SP(OMe)R*}(CO)$_2$] in similar amounts. Other electrophiles added selectively to the terminal O atom of the R*POS ligand. Thus the thiooxophosphorane complex reacted with ClC(O)C$_2$H$_3$, [NH$_4$]PF$_6$, ClSiMe$_3$, ClSnMe$_3$ and [ZrCp$_2$Cl$_2$] to give the corresponding derivatives [MoCp{*S,P*-SP(OX)R*}(CO)$_2$] (X = C(O)C$_2$H$_3$, H, SiMe$_3$, SnMe$_3$, ZrCp$_2$Cl). The structure of two of these products (X = C(O)C$_2$H$_3$, SiMe$_3$) was determined by single-crystal X-ray diffraction studies. Density functional theory (DFT) calculations of the title anions and some of their derivatives indicated that attachment of an external electrophile to the terminal O atom of the thiooxophosphorane ligand is favoured under conditions of charge control, while the sulphur atom is the favoured site under conditions of orbital control, although it leads to less stable products.

Introduction

Dioxophosphoranes (RPO$_2$) and thiooxophosphoranes (RPOS) are unstable molecules generated during thermolysis of a great variety of suitable organophosphorus precursors. These transient molecules display a strongly electrophilic character located at their positively-polarized phosphorus(V) atom, this enabling their use as strong phosphorylating agents upon reaction with many different organic substrates while, in the absence of external reagents, they usually evolve through polymerization or intramolecular activation of C–H bonds.[1] Only under very favourable conditions can these species be detected directly, as it is the case of MePO$_2$ when generated in the gas phase under high vacuum.[2] It might be conceived that substantial stabilization of these elusive molecules could be achieved through coordination to metal centres, which in turn would allow for a more detailed study of their chemical behaviour. However, the coordination chemistry of these molecules is virtually unknown, with just one example described for a dioxophosphorane complex.[3] In a preliminary study we found that the anionic oxophosphinidene complex (H-DBU)[MoCp(CO)$_2${P(O)R*}] (**1**), (R* = 2,4,6-C$_6$H$_2$^{t}Bu$_3$; Cp= η^5-C$_5$H$_5$, DBU = 1,8-diazabicyclo[5.4.0]undec-7-ene), could be used as a precursor for the corresponding dioxophosphorane (H-DBU)[MoCp(CO)$_2${*O,P*-OP(O)R*}] (**2**) and thiooxophosphorane (H-DBU)[MoCp(CO)$_2${*S,P*-SP(O)R*}] (**3**) derivatives (Scheme 1).[4] Because of the negative charge of the latter complexes, the acid-base chemistry of their phosphorus ligands is reversed, so they can now behave as nucleophiles. Indeed our preliminary study on the reactivity of the thiooxophosphorane complex **3** indicated that methylation could occur easily at either the S and O sites, to give unprecedented thiolophosphinide (PR(O)(SMe)) and phosphonothiolate (PR(OMe)S) derivatives, respectively.[4] Therefore it was of interest exploring the potential of anions **2** and **3** in the generation of novel P-donor entities. In this paper we give full details of the above reactions, which we have now extended to the dioxophosphorane complex **2** and also to other electrophilic reagents, including the proton and some metal-based electrophiles. As it will be shown, most electrophiles add to the terminal oxygen atom of the phosphorus ligand of the

above anions, an event favoured on steric, electrostatic and thermodynamic grounds, according to our theoretical calculations. Addition to the sulphur site of the thiooxophosphorane ligand is an orbital-favoured event only observed in the methylation reactions of **3**.

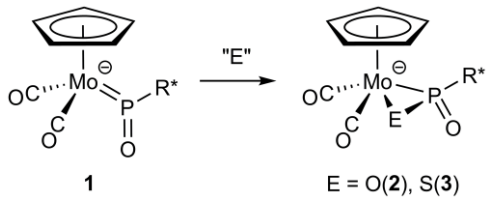

Scheme 1

Results and Discussion

Synthesis and structure of dioxo- and thiooxophosphorane complexes

The oxophosphinidene complex **1** reacts readily at 243 K with a mild oxygenating reagent as dimethyldioxirane to yield the corresponding dioxophosphorane derivative (H-DBU)[MoCp(CO)$_2${*O*,*P*-OP(O)R*}] (**2**) as major product. This compound, however, was quite air-sensitive and could not be obtained as a pure material, although it could be used for further reactions. In a related way, **1** reacts rapidly at 273 K with S_8 to give the thiooxophosphorane derivative (H-DBU)[MoCp(CO)$_2${*S*,*P*-SP(O)R*}] (**3**), a more stable species that could be isolated as a pure material in a conventional way. These reactions can be easily extended to the tungsten analogue of **1**. Thus, the latter reacts with S_8 to give the corresponding tungsten derivative (H-DBU)[WCp(CO)$_2${*S*,*P*-SP(O)R*}] (**3´**) in good yield. The formation of the above compounds can be viewed as resulting from addition of a chalcogen atom (E) to the Mo=P bond *via* the HOMO of the starting oxophosphinidene complex, which has π(Mo–P) bonding character and displays lobes oriented perpendicular to the Mo–P–O plane,[5] and is thus expected to leave the newly incorporated atom E nearly perpendicular to that plane (Scheme 1), in agreement with the calculations on **2** and **3** described below.

Table 1. Selected IR[a] and $^{31}P\{^1H\}$NMR[b] Data for New Compounds.

Compound	ν(CO)	δ_P (J_{PW})
(H-DBU)[MoCp(CO)$_2${P(O)R*}] (**1**)[c]	1874 (vs), 1790 (s)[d]	385.0
(H-DBU)[WCp(CO)$_2${P(O)R*}] (**1´**)[c]	1868 (vs), 1784 (s)	335.6 (658)
(H-DBU)[MoCp(CO)$_2${*O*,*P*-OP(O)R*}] (**2**)	1904 (vs), 1803 (s)	39.6
(H-DBU)[MoCp(CO)$_2${*S*,*P*-SP(O)R*}] (**3**)	1911 (vs), 1816 (s)	83.8
(H-DBU)[WCp(CO)$_2${*S*,*P*-SP(O)R*}] (**3´**)	1902 (vs), 1803 (s)	43.3 (240)
[MoCp{*O*,*P*-OP(OMe)R*}(CO)$_2$] (**4**)	1948 (vs), 1856 (s)	73.1
[MoCp{*S*,*P*-(MeS)P(O)R*}(CO)$_2$] (**5**)	1963 (vs), 1887 (s)	102.0
[MoCp{*S*,*P*-SP(OMe)R*}(CO)$_2$] (**6**)	1947 (vs), 1862 (s)	122.0
[MoCp{*S*,*P*-SP(OC(O)C$_2$H$_3$)R*}(CO)$_2$] (**7**)	1961 (vs), 1879 (s)	107.4
[MoCp{*S*,*P*-SP(OH)R*}(CO)$_2$] (**8**)	1950 (vs), 1862 (s)	101.2[e]
[MoCp{*S*,*P*-SP(OSiMe$_3$)R*}(CO)$_2$] (**9**)	1946 (vs), 1858 (s)	97.0
[MoCp{*S*,*P*-SP(OSnMe$_3$)R*}(CO)$_2$] (**10**)	1935 (vs), 1843 (s)	101.0
[MoCp{*S*,*P*-SP(OZrCp$_2$Cl)R*}(CO)$_2$] (**11**)	1938 (vs), 1846 (s)	106.0

[a] Recorded in dichloromethane solution, with C–O stretching bands [ν(CO)] in cm^{-1}. [b] Recorded in CD_2Cl_2 at 121.50 MHz and 295 K, with ^{31}P-^{183}W coupling constants (J_{PW}) in Hz. [c] Data taken form reference 5; DBU = 1,8-diazabicyclo[5.4.0]undec-7-ene. [d] Recorded in tetrahydrofuran solution. [e] Recorded at 162.01 MHz and 263 K.

Spectroscopic data in solution for compounds **2**, **3** and **3´** (Table 1 and Experimental Section) are fully consistent with the structure proposed for the corresponding anions. As expected, these complexes display C–O stretches in the IR spectrum at frequencies higher than the starting material, and with a similar pattern (very strong and strong, in order of decreasing frequencies), this being characteristic of M(CO)$_2$ oscillators with C–M–C angles somewhat lower than 90°.[6] It is perhaps surprising (based on the relative electronegativity of O *vs*. S) that the dioxophosphorane **2** displays bands some 10 cm^{-1} lower than the thiooxophosphorane analogue **3**, which indicates a more efficient electron donation from the *O*,*P*-bound dioxophosphorane ligand to the metal centre.

Upon addition of the chalcogen atom to the oxophosphinidene ligand, the P nucleus undergoes a dramatic nuclear shielding of some 300 ppm, consistent with a change from planar trigonal to a distorted tetrahedral environment (Table 1). We note that the chemical shift of **2** is very close to those measured for the only other dioxophosphorane complexes described in the literature (δ_P *ca.* 40 ppm for [Ru(η^6-*p*-cymene){*O*,*P*-OP(O)R*}(PR$_3$)]; R = Ph, Cy).[3] At the same time, the P–W coupling in the tungsten derivative **3´** is more than halved with respect to its precursor **1´**, thus reflecting the

increased coordination number of the P and W atoms and formal reduction in W–P bond order (from 2 to 1).[7] Because of the absence of any symmetry elements in these molecules, their ^{1}H and ^{13}C NMR spectra display separated resonances for the pairs of CO ligands, CH(aryl) moieties or *ortho*-^{t}Bu substituents, often exhibiting substantial differences in the corresponding couplings to the P atom. Such differences are particularly strong for the carbonyl ligands, due to their distinct positioning (hence different C–M–P angles) with respect to the P atom (e.g. 29 *vs.* ~0 Hz for J_{PC} in **3**).[8] These spectroscopic features are also present in all neutral derivatives of anions **2** and **3** and will not be further discussed.

In order to gain further support for the structure of these anions and to better understand their reactivity toward different electrophiles we have computed the geometric and electronic structure of the anions in **2** and **3** using density functional theory (DFT) methods.[9] We have also inspected the topological properties of the electron density as managed by the atoms in molecules (AIM) theory.[10] First we note that the optimized structures of these anions (Figure 1 and Table 2) are as expected from the considerations given above. Thus, the short Mo=P distance of 2.287 Å in **1** is enlarged to values of ca. 2.50 Å, consistent with single Mo–P bonds, while the terminal P=O bond lengths of 1.51 Å have remained almost unperturbed (cf. 1.518 Å in **1**),[5] and consistent with a considerable multiple bond character, close to a formal order of two. We note that the computed P–O lengths for free P(O)R* (1.501 Å),[5] and $MePO_2$ (1.461 Å),[2] are only slightly shorter than the above figures. In contrast, the P–O length for the Mo-bound oxygen in **2** is substantially longer, as expected for an interaction approaching the single-bond character. We finally note that the Mo–P length in the dioxophosphorane complex **2** is ca. 0.07 Å shorter than the corresponding distance in the thiooxophosphorane **3**, suggesting a stronger binding of the $R^{*}PO_2$ ligand to the metal centre, in agreement with the lower C–O frequencies of **2** noted above.

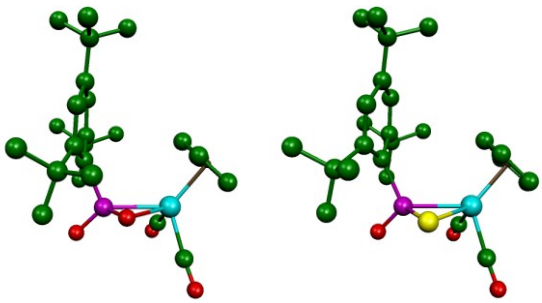

Figure 1: DFT-optimized structures of the anions in compounds **2** (left) and **3** (right), with H atoms omitted for clarity.

Table 2. Selected Bond lengths (Å) and Angles (°) for DFT-Optimized Geometries.

Parameter	**1**[a]	**2**	**3**	**5**	**6**	**8-S**	**8-O**
Mo–P	2.287	2.472	2.536	2.514	2.478	2.508	2.470
Mo–E		2.227	2.592	2.578	2.617	2.587	2.620
P–E		1.580	2.094	2.283	2.049	2.343	2.046
P=O/ P–OC/H	1.518	1.509	1.516	1.506	1.647	1.501	1.655
Mo–E–P		78.9	64.5	64.8	62.8	60.9	62.5
E–P–Mo		62.2	67.3	64.8	69.9	64.3	70.2
P–Mo–E		38.9	48.2	53.2	47.3	54.7	47.3
Mo–P–O	136.0	131.9	128.2	125.6	125.8	125.8	121.1
E–P–O		120.1	119.2	110.1	112.0	112.0	112.3
OC–Mo–CO	85.0	80.5	79.7	79.5	79.9	79.4	79.8
OC–Mo–P	89.4	84.1	82.4	80.7	88.5	80.4	87.2
OC–Mo–P	90.7	103.2	104.7	108.0	106.3	106.6	106.7

[a] Data taken from reference 5.

Inspection of the topology of electron density involving the EP(O)R* ligands in anions **2** and **3** gives a picture consistent with that derived from the above geometrical analysis (see the Supplementary Information). Thus, the electron density (ρ) at the corresponding Mo–P bond critical points (bcp) follows the expected order (0.636 (**1**) >> 0.488 (**2**) > 0.463 (**3**) eÅ^{-3}), while that at the terminal P=O bond remains with a high value of 1.40-1.43 eÅ^{-3} (cf. 1.431 eÅ^{-3} in **1**) and with a very high value of *ca.* 35 eÅ^{-5} for its Laplacian ($\nabla^2\rho$), which is a feature characteristic of multiple CO bonds in organic molecules and transition-metal carbonyls.[11] In contrast, the P–O bond for the Mo-bound O atom displays a lower electron density at the corresponding bcp (1.240 eÅ^{-3}), with a negative value for its Laplacian (–17.6 eÅ^{-5}), as expected for a covalent single bond.

As concerning the Lewis-base behaviour of compounds **2** and **3**, atomic charges and occupied frontier orbitals are the major items to look at. The relevant atomic charges computed for **2** and **3** are collected in Table 3, these including Mulliken charges,[12] and those derived from the NBO analysis (NPA charges).[13] Both schemes give a similar picture: a high and comparably negative charge at both O atoms in **2**, and a negative charge much higher at O than at the S atom for the thiooxophosphorane complex **3**. Thus we conclude that, under conditions of charge control, compound **2** might not display a

particular site preference for attachment of an incoming electrophile, but the thiooxophosphorane complex **3** should display a definite preference for attachment at the terminal O site, which moreover is likely a more accessible site on steric grounds. The frontier orbitals of these anions (see the Supplementary Information) are not very different from each other, except for the corresponding HOMO, which is largely located at the metal site in the anion of **2**, whereas it has a large contribution from a sulphur lone pair in the anion of **3** (Figure 2), thus enabling in the latter case the attachment of an incoming electrophile at the sulphur position under conditions of orbital control.

Table 3. Selected Atomic Charges for the Anions of **2** and **3**.

Atom	2		3	
	Mulliken	NPA	Mulliken	NPA
Mo	–0.151	–0.138	–0.4706	–0.349
E	–0.671	–0.983	–0.266	–0.485
P	1.080	1.874	0.832	1.424
O(term)	–0.615	–1.081	–0.604	–1.072

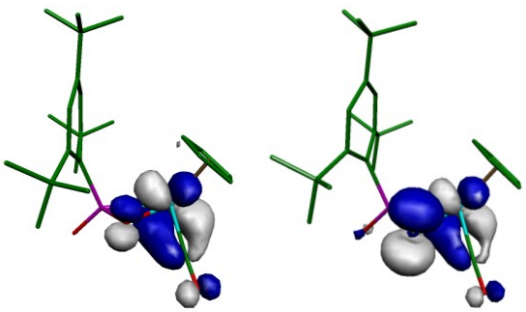

Figure 2: DFT-computed HOMO orbitals for the anions in compounds **2** (left) and **3** (right).

Methylation and related reactions of complexes 2 and 3

The dioxophosphorane complex **2** failed to react with the soft methylating agent MeI at room temperature, but reacts readily with the stronger reagent $(Me_3O)BF_4$ to give selectively the phosphonite complex [MoCp{*O*,*P*-OP(OMe)R*}$(CO)_2$] (**4**), a derivative formally resulting from selective attachment of the Me^+ cation to the terminal O atom of the former dioxophosphorane ligand (Chart 1). In contrast, methylation of the thiooxophosphorane complex **3** is strongly dependent on the electrophilic reagent used. Thus, its reaction with MeI takes place selectively at the sulphur site to give the thiolophosphinide derivative [MoCp{*S*,*P*-(MeS)P(O)R*}$(CO)_2$] (**5**), whereas its reaction with $(Me_3O)BF_4$ yields a mixture of **5** and the phosphonothiolate complex [MoCp{*S*,*P*-SP(OMe)R*}$(CO)_2$] (**6**) in similar amounts, with the latter resulting from attachment of the Me^+ cation to the oxygen atom of the thiooxophosphorane ligand. In view of the considerations made above, it is clear that **5** is the product of orbital control, and thus is preferentially formed when using soft methylating reagents, whereas **6** emerges under conditions of charge control. In reactions of the dioxophosphorane **2**, interaction with the incoming electrophile is probably dominated by electrostatic factors and, since both oxygen atoms of the R^*PO_2 ligand bear comparable negative charges, the reason for the observed selective methylation at the terminal O site would be the superior accessibility of that site to an external reagent. In line with this hypothesis, we note that reaction of **3** with acryloyl chloride gives exclusively the corresponding phosphonothiolate derivative [MoCp{*S*,*P*-SP(OC(O)C_2H_3)R*}$(CO)_2$] (**7**), here suggesting the operation of steric barriers disfavouring the approach of an external reagent, certainly softer than $(Me_3O)BF_4$, to the S site.

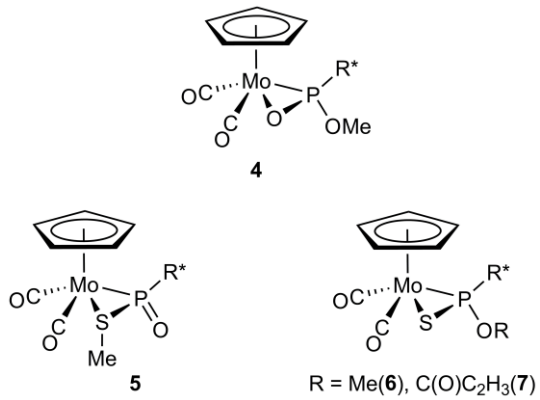

Chart 1

Structure of phosphonite and phosphonothiolate derivatives

The structure of the *O*-methylated derivative **6** was established during our preliminary study of the reactivity of **3**.[4] We have now determined the structure of the related complex **7**, which displays comparable geometrical parameters (Figure 3 and Table 4). The salient feature of this structure is the presence of an *S*,*P*-bound phosphonothiolate ligand derived from attachment of the hydrocarbyl group at the O-site of the thiooxophosphorane ligand of **3**. As a result, the P–O distance (1.656(1) Å) becomes much longer than the distance of 1.516 Å computed for the P=O bond in **3** (Table 2), as expected for a single bond between these atoms. In contrast, the P–S bond (2.0022(6) Å) becomes slightly shorter than the corresponding length computed for **3** (2.094 Å), and it should be considered as relatively short for a P–S single bond (expected around 2.12 Å).[14] Similarly short P–S lengths have been found previously for different *S*,*P*:*P*-bridged chalcogenophosphinidene Mo_2 complexes, a circumstance which we have linked to the involvement of the chalcogen atom in some π(S–P) bonding interaction within the MoPS ring of these molecules.[15] On the other hand, the Mo–P bond of **3** is neither expected to be much perturbed upon alkylation, and displays a value of 2.3963(6) Å, indicative of a strong single bond. A final structural feature deserved of comment is the distorted trigonal pyramidal environment around the P atom, derived from the fact that this atom remains placed almost in the same plane as the Mo, O3 and C11 atoms (Σ(X–P–Y) = 354°). Although no *S*,*P*-bound

phosphonothiolate complex other than **6** has been structurally characterized, we note that this local environment is also present in related *O*,*P*-bound phosphinite and phosphonite complexes,[4,5] and also in the *S*,*P*-bound thiophosphinite (or phosphinothiolate) complexes $[WCp(SPCl^tBu)(CO)_2]$,[16] $[WCp\{SPMeN(SiMe_3)_2\}(CO)_2]$[17] and $[Mo(C_6H_7)(SPMe_2)(CO)_2]$.[18]

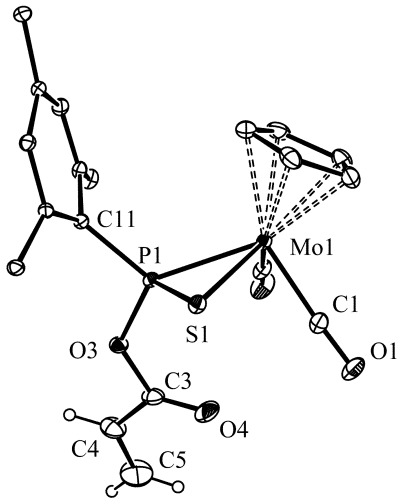

Figure 3: ORTEP diagram (30% probability) of compound **7** with H atoms (except the olefinic ones) and ^{t}Bu groups (except their C1 atoms) omitted for clarity.

Table 4: Selected Bond Lengths (Å) and Angles (deg) for Compound **7**.

Mo1–P1	2.3963(6)	C1–Mo1–C2	76.5(1)
Mo1–S1	2.5570(6)	P1–Mo1–C1	105.2(1)
Mo1–C1	1.968(2)	P1–Mo1–C2	86.8(1)
Mo1–C2	1.956(2)	P1–Mo1–S1	47.55(2)
P1–S1	2.0022(6)	P1–S1–Mo1	62.01(2)
P1–O3	1.656(1)	Mo1–P1–S1	70.44(2)
P1–C11	1.830(2)	Mo1–P1–O3	128.66(4)
O3–C3	1.380(2)	P1–O3–C3	126.0(1)
C3–O4	1.186(2)	O3–C3–O4	123.7(2)
C4–C5	1.309(3)	O3–C3–C4	109.4(2)

Spectroscopic data in solution for the phosphonothiolate complexes **6** and **7** (Table 1 and Experimental Section) are fully consistent with their asymmetric solid-state structures and deserve no particular comment. We just note that they display ^{31}P NMR resonances some 30 ppm more deshielded than that of the starting anion **3**, while their C–O stretches are substantially more energetic, as expected from the reduction of charge in these neutral derivatives. As for the phosphonite complex **4**, all data point to an *O*,*P*-bound structure similar to that of the sulphur-containing analogues **6** and **7**. Actually, such a coordination geometry has been confirmed crystallographically for $[MoCp\{O,P\text{-}OP(OC_6H_4OH)R^*\}(CO)_2]$,[4] a complex resulting from reaction of **1** with *p*-benzoquinone, which incidentally remains as the only *O*,*P*-bound phosphonite complex structurally characterized so far. Spectroscopic data for the latter complex are indeed comparable to those of **4**, particularly its C–O stretches (1945 (vs), 1865 (s) cm^{-1}) and ^{31}P chemical shift (δ_P 74.5 ppm, *cf.* 73.1 ppm for **4**), which again are some 30 ppm higher than that of the parent anion **2**.

Structure of the thiolophosphinide complex 5

The structure of the *S*-methylated derivative **5** also was established during our preliminary study of the reactivity of **3** (Figure 4).[4] No other complex containing a comparable ligand seems to have been structurally characterized so far. As a result of the attachment of the methyl group to the sulphur atom of **3**, any π-bonding interaction involving the S atom vanishes, and accordingly the P–S length in **5** is elongated to a value of 2.1805(6) Å, while the P–O bond is little perturbed as judged from the corresponding bond length, which remains short (1.492(3) Å) and comparable to the corresponding figure computed for **3**. The general environment around the P atom also is little perturbed, with the Mo, P, O and C31 atoms remaining almost coplanar (Σ(X–P–Y) = 359°), as found also for the isomeric phosphonothiolate complexes **6** and **7**. As expected, the *S*-bound methyl group points away from the bulky R* substituent at phosphorus, thus yielding a less congested diastereoisomer.

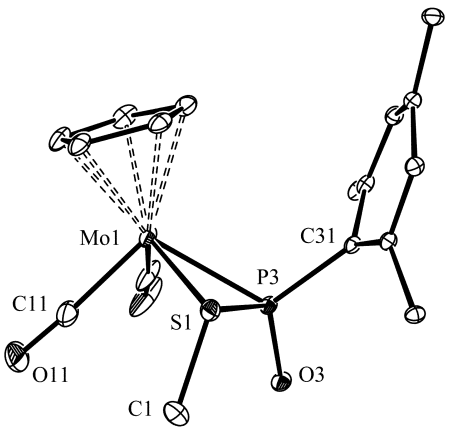

Figure 4: ORTEP diagram (30% probability) of compound **5** with H atoms and ^{t}Bu groups (except their C1 atoms) omitted for clarity.[4] Selected bond lengths (Å) and angles (°): Mo1–P3 = 2.4415(5); Mo1–S1 = 2.4939(5); P3–S1 = 2.1805(6); P3–O3 = 1.492(1); P3–C31 = 1.847(1). C11–Mo1–C12 = 78.4(1).

In order to find the relative stability of the phosphonothiolate or thiolophosphinide derivatives of **3** we computed the structures of isomers **5** and **6** using DFT methods. The minimized structures (Table 2 and Supporting Information) were in good agreement with those determined crystallographically, although the computed bond lengths involving the Mo atoms were somewhat longer than the experimental data, a common trend of the functionals currently used in DFT computations of transition metal complexes,[9a,19] and the P–S length for **5** also was significantly longer than the experimental value (2.283 *vs.* 2.1805(6) Å). The Gibbs free energy computed for the thiolophosphinide complex **5** was 21 kJ/mol above that of its isomer **6**, then qualifying it as a kinetic

product. This energetic difference perhaps is mainly derived from the different strength of the new bonds being formed in each case (the S–C bond energy is some 85 kJ/mol lower than that of an O–C bond).[20] Moreover, the electron donation of the phosphonothiolate ligand of **6** seems to be more efficient than that of the isomeric thiolophosphinide ligand in **5**, as judged from the respective C–O stretching frequencies, which are some 15 cm^{-1} lower for **6** (Table 1).

Protonation of compound 3

The thiooxophosphorane ligand in **3** is readily protonated upon reaction with a weak acid as $[NH_4]PF_6$ in dichloromethane solution, to give the corresponding neutral derivative [MoCp{*S*,*P*-SP(OH)R*}$(CO)_2$] (**8**) as unique product, a process that can be quantitatively reversed upon reaction of the latter with DBU. This quite air-sensitive complex displays C–O stretching bands almost identical to those of the *O*-methylated derivative **6**, with frequencies significantly lower than those of the *S*-methylated derivative **5**, thus suggesting that the added proton is attached to the terminal O site of the anion of **3**, rather than attached to the sulphur atom (Chart 2). The appearance of a broad resonance at *ca.* 6.8 ppm in the ^{1}H NMR spectrum of **8** also supports the presence of an OH group.

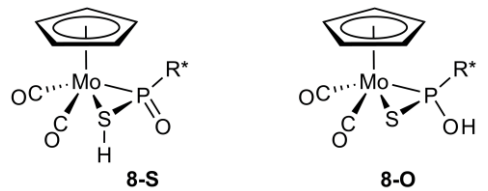

8-S **8-O**

Chart 2

Further support for the proposed structure for **8** was obtained by computing the gas-phase structures of the *S*-protonated (**8-S**) and *O*-protonated (**8-O**) derivatives of the anion of **3** (see Table 2 and Supplementary Information). Indeed the computed structures are very similar to those of the methylated products **5** and **6** respectively (Table 2), and the Gibbs free energy for **8-S** now is much higher (by 51 kJ/mol) than that of **8-O**, once more reflecting the relative strengths of the newly formed bonds (the S–H bond energy is some 95 kJ/mol lower than that of a O–H bond).[20] We should stress that no other complex containing a thiolophosphonous (or phosphonothious) acid ligand (PR(OH)(SH)) or any of their conjugated anions appears to have been reported in the literature.

Heterometallic derivatives of compound 3

We have shown previously that reactions of the oxophosphinidene complex **1** with metal-based electrophiles may lead to products resulting from attachment of the added electrophile to the terminal O atom of the phosphorus ligand, to give oxophosphinidene-bridged derivatives, or to the metal atom of the anion, to give products with new heterometallic Mo–M bonds, with the latter being the preferred outcome when using soft electrophiles.[21] We have now examined reactions of the thiooxophosphorane complex **3** with analogous reagents which, by taking into account the outcome of the methylation and protonation reactions discussed above, might be expected to take place at either the S or O atoms of the anion. However, these reactions instead turned to occur selectively at the terminal O atom of the anion irrespective of the electrophile being used.

Compound **3** reacts readily with the relatively hard electrophiles $SiMe_3Cl$, $SnMe_3Cl$ and $[ZrCp_2Cl_2]$ to give the corresponding phosphonothiolate-like derivatives [MoCp{*S*,*P*-SP$(OSiMe_3)$R*}$(CO)_2$] (**9**), [MoCp{*S*,*P*-SP$(OSnMe_3)$R*}$(CO)_2$] (**10**) and [MoCp{*S*,*P*-SP$(OZrCp_2Cl)$R*}$(CO)_2$] (**11**), all of them displaying a thiooxophosphorane ligand bridging the metal atoms in a novel μ-*S*,*P*:*O*- fashion (Chart 3). Reactions with softer electrophiles such as the Au(I) complexes $[Au(THT)(PR_3)]PF_6$ (R = Ph, Me; THT = SC_4H_8) yielded similar derivatives, as judged from the corresponding IR and NMR spectra, but these products were quite unstable and could not be properly isolated and characterized.

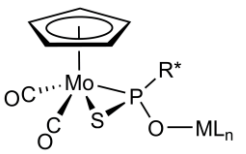

	ML_n
9	$SiMe_3$
10	$SnMe_3$
11	$ZrCp_2Cl$

Chart 3

The structure of the silyl derivative **9** in the crystal (Figure 5 and Table 5) is very similar to those determined for the hydrocarbyl derivatives **6** and **7** and need not to be discussed in detail, except for the P–O–Si linkage, which displays a relatively large P–O–Si angle of 146.6° (cf. 126° for the analogous P–O–C angle in **7**), and a P–O length slightly shorter than that in **7** (1.579(4) *vs.* 1.656(1) Å). This is not unusual in the chemistry of silicon, and might be associated with some participation of the lone electron pairs at oxygen in π bonding along the P–O–Si chain, while at the same time alleviating the steric pressure around the P atom. For instance, in the *cis* and *trans* isomers of the complex $[PdCl_2\{P(OSiMe_3)_3\}_2]$ the P–O lengths fall in the range 1.55-1.57 Å (O–Si lengths *ca.* 1.67 Å), while the P–O–Si angles span a wide range of 136-152°.[22] In the same line, the tungsten complex $[W(CO)_5\{PH(OSiMe_3)(CH(SiMe_3)_2)\}]$ displays values of *ca.* 1.60 Å and 142° for these geometrical parameters.[23]

Spectroscopic data in solution for compounds **9** to **11** (Table 1 and Experimental Section) are fully consistent with the structure found for **9** in the crystal, and are comparable to those of the phosphonothiolate complexes **6** and **7**, then deserving no detailed analysis. We just note that the C–O stretching frequencies of these complexes broadly reflect the expected trend based on the electron withdrawing power of the electrophile being attached to the O atom of the phosphorus ligand, by following the sequence **6** (CH_3) > **9** ($SiMe_3$) >> **11** ($ZrCp_2Cl$) > **10** ($SnMe_3$). The relative order of the tin and zirconium derivatives is not the expected one on the basis of relative electronegativities of Sn and Zr, and probably reflects a

superior involvement of the latter atom in a π(O→Zr) interaction that in the end would remove electron density off the molybdenum centre.

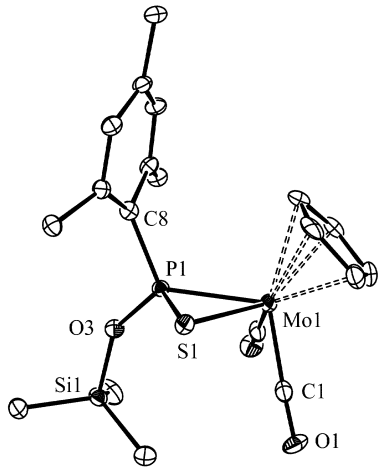

Figure 5: ORTEP diagram (30% probability) of compound **9** with H atoms and ^{t}Bu groups (except their C1 atoms) omitted for clarity

Table 5: Selected Bond Lengths (Å) and Angles (deg) for Compound **9**.

Mo1–P1	2.417(2)	C1–Mo1–C2	80.3(3)
Mo1–S1	2.544(2)	P1–Mo1–C1	107.3(2)
Mo1–C1	1.956(7)	P1–Mo1–C2	84.6(2)
Mo1–C2	1.973(7)	P1–Mo1–S1	47.74(5)
P1–S1	2.011(2)	P1–S1–Mo1	62.82(6)
P1–O3	1.579(4)	Mo1–P1–S1	69.45(6)
P1–C8	1.838(6)	Mo1–P1–O3	127.1(2)
O3–Si1	1.680(4)	P1–O3–Si1	146.6(3)

Conclusions

The formation of the title compounds can be viewed as resulting from addition of a chalcogen atom (E) to the Mo=P bond in the parent oxophosphinidene complex $[MoCp(CO)_2\{P(O)R^*\}]^-$ *via* the HOMO of the latter, which displays lobes oriented perpendicular to the Mo–P–O plane, and is thus expected to leave the newly incorporated atom E nearly perpendicular to that plane, in agreement with their DFT-optimized structures. The thiooxophosphorane complex **3** bears a negative charge at O much higher than that at the S atom, while its HOMO has a large contribution from a sulphur lone pair. This favours the attachment of an incoming electrophile to the sulphur atom under conditions of orbital control, thus explaining the selective formation of the thiolophosphinide complex **5** in the reaction of **3** with the soft reagent MeI. In contrast, attachment of the incoming electrophile to the O atom is favoured under conditions of charge control and is also kinetically favoured on steric grounds, thus explaining the preferential or specific formation of phosphonothiolate and related complexes in the reactions of **3** with all other electrophilic reagents investigated in this work. According to our DFT calculations on the H^+ and Me^+ derivatives of **3**, the phosphonothiolate complexes invariably are thermodynamically favoured over their thiolophosphinide isomers, likely as a result of the considerably higher strength of the newly formed O–H and O–C bonds, relative to the alternative formation of S–H and S–C bonds.

Acknowledgments

We thank the DGI of Spain and the Consejería de Educación del Principado de Asturias for financial support (Projects CTQ2012-33187 and IB05-110), and the MEC of Spain for a grant (to M. A.). We also thank the CMC of the Universidad de Oviedo for access to computing facilities, and the X-Ray units of the Universidad de Oviedo and Universidad de Santiago de Compostela for acquisition of diffraction data.

Experimental Section

General procedures and starting materials

All manipulations and reactions were carried out under a nitrogen (99.995%) atmosphere using standard Schlenk techniques. Solvents were purified according to literature procedures, and distilled prior to use.[24] Compounds (H-DBU)[MoCp{P(O)R*}(CO)$_2$] (**1**) and (H-DBU)[WCp{P(O)R*}(CO)$_2$] (**1´**) (R* = 2,4,6-$C_6H_2{}^tBu_3$; Cp = η^5-C_5H_5; DBU = 1,8-diazabicyclo[5.4.0]undec-7-ene),[5] and dimethyldioxirane,[25] were prepared as described previously, and all other reagents were obtained from the usual commercial suppliers and used as received, unless otherwise stated. Petroleum ether refers to that fraction distilling in the range 338-343 K. Filtrations were carried out through diatomaceous earth unless otherwise indicated. Chromatographic separations were carried out using jacketed columns refrigerated by tap water (*ca.* 288 K) or by a closed 2-propanol circuit kept at the desired temperature with a cryostat. Commercial aluminium oxide (activity I, 150 mesh) was degassed under vacuum prior to use. The latter was mixed afterward under nitrogen with the appropriate amount of water to reach the activity desired (activity IV, unless otherwise stated). IR stretching frequencies of CO ligands were measured in solution, using CaF_2 windows. Nuclear Magnetic Resonance (NMR) spectra were routinely recorded at 300.13 (^{1}H), 121.50 (^{31}P{^{1}H}) or 75.47 MHz (^{13}C{^{1}H}) at 295 K in CD_2Cl_2 solution unless otherwise stated. Chemical shifts (δ) are given in ppm, relative to internal tetramethylsilane (^{1}H, ^{13}C) or external 85% aqueous H_3PO_4 (^{31}P). Coupling constants (J) are given in Hertz.

Preparation of (H-DBU)[MoCp(CO)$_2${*O*,*P*-OP(O)R*}] (2). Dimethyldioxirane (1.0 mL of a *ca.* 0.1 M solution in acetone, 0.10 mmol) was added to a dichloromethane solution (10 mL) of compound **1** (0.030 g, 0.045 mmol) at 243 K, and the mixture was stirred for 20 min to give an orange solution. The solvent was then removed under vacuum, the residue was extracted with diethyl ether (15 mL) and the extract filtered using a cannula. Removal of solvent from the filtrate and washing of the residue with petroleum ether gave compound **2** as an air-sensitive, reasonably pure orange powder

(0.016 g, 52 %). Attempts to further purify this product resulted in its progressive decomposition. ^{1}H NMR (200.13 MHz): δ 11.78 (s, 1H, NH), 7.34 (dd, J_{HP} = 5, J_{HH} = 2, 1H, C_6H_2), 7.24 (t, J_{HP} = J_{HH} = 2, 1H, C_6H_2), 4.81 (s, 5H, Cp), 3.47-3.20 (m, 6H, CH_2), 2.79, 1.96 (2m, 2 x 2H, CH_2), 1.76, 1.52, 1.32 (3s, 3 x 9H, ^{t}Bu), 1.75-1.64 (m, 6H, CH_2).

Preparation of (H-DBU)[MoCp(CO)$_2${*S*,*P*-SP(O)R*}] (3). Sulphur (0.73 mL of a *ca.* 0.062 N solution in dichloromethane, 0.045 mmol) was added to a dichloromethane solution (10 mL) of compound **1** (0.030 g, 0.045 mmol) at 273 K, and the mixture was stirred for 2 min to give an orange solution. Solvent was then removed under vacuum, the residue extracted with diethyl ether (2 x 10 mL) and the extracts filtered. Removal of solvent from the filtrate and washing of the residue with petroleum ether gave compound **3** as an orange powder (0.029 g, 93%). Anal. Calcd for $C_{34}H_{51}MoN_2O_3PS$: C, 58.78; H, 7.40; N, 4.03. Found: C, 59.34; H, 7.17; N, 4.12. ^{1}H NMR: δ 12.28 (s, 1H, NH), 7.21 (dd, J_{HP} = 5, J_{HH} = 2, 1H, C_6H_2), 7.09 (t, J_{HP} = J_{HH} = 2, 1H, C_6H_2), 4.71 (s, 5H, Cp), 3.38-3.28 (m, 6H, CH_2), 2.75, 1.94 (2m, 2 x 2H, CH_2), 1.76-1.61 (m, 6H, CH_2), 1.71, 1.64, 1.28 (3s, 3 x 9H, ^{t}Bu). ^{13}C{^{1}H} NMR: δ 254.6 (d, J_{CP} = 29, MoCO), 247.1 (s, MoCO), 165.7 (s, CN), 156.4 [d, J_{CP} = 21, $C^2(C_6H_2)$], 153.7 [s, $C^4(C_6H_2)$], 148.4 [s, $C^2(C_6H_2)$], 144.1 [d, J_{CP} = 46, $C^1(C_6H_2)$], 121.7 [d, J_{CP} = 10, $C^3(C_6H_2)$], 120.4 [d, J_{CP} = 15, $C^3(C_6H_2)$], 94.2 (s, Cp), 53.2, 47.9, 38.2, 32.0, 29.0, 26.7, 24.4, 19.4 (8s, CH_2), 41.5, 40.1, 34.7 [3s, $C^1(^t$Bu)], 34.8, 34.3, 31.2 [3s, $C^2(^t$Bu)].

Preparation of (H-DBU)[WCp(CO)$_2${*S*,*P*-SP(O)R*}] (3´). The procedure is analogous to that described for compound **3**, but using compound **1´** (0.030 g, 0.040 mmol) as starting material. After similar workup, compound **3´** was obtained as an orange solid (0.030 g, 96%). Anal. Calcd for $C_{34}H_{51}N_2O_3PSW$: C, 52.18; H, 6.57; N, 3.58. Found: C, 52.44; H, 6.38; N, 3.49. ^{1}H NMR (200.13 MHz): δ 12.11 (s, 1H, NH), 7.21 (dd, J_{HP} = 5, J_{HH}= 2, 1H, C_6H_2), 7.10 (t, J_{HP} = J_{HH}= 2, 1H, C_6H_2), 4.80 (s, 5H, Cp), 3.43-3.30 (m, 6H, CH_2), 2.78, 1.95 (2m, 2 x 2H, CH_2), 1.77-1.70 (m, 6H, CH_2) 1.73, 1.64, 1.28 (3s, 3 x 9H, ^{t}Bu).

Preparation of [MoCp{*O*,*P*-OP(OMe)R*}(CO)$_2$] (4). Solid $(Me_3O)BF_4$ (0.010 g, 0.067 mmol) was added to a dichloromethane solution (10 mL) of compound **2** (0.040 g, 0.059 mmol) at 273 K, and the mixture was stirred for 5 min to give an orange solution. Solvent was then removed under vacuum and the residue was chromatographed on alumina at 253 K. Elution with dichloromethane/petroleum ether (1/9) gave a pink fraction yielding, after removal of solvents, compound **4** as an orange solid (0.029 g, 91%). Anal. Calcd for $C_{26}H_{37}MoPO_4$: C, 57.78; H, 6.90. Found: C, 57.54; H, 7.04. ^{1}H NMR: δ 7.47 (dd, J_{HP} = 6, J_{HH} = 2, 1H, C_6H_2), 7.37 (t, J_{HP} = J_{HH} = 2, 1H, C_6H_2), 5.05 (s, 5H, Cp), 3.44 (d, J_{HP} = 14, 3H, OMe), 1.64, 1.45, 1.33 (3s, 3 x 9H, ^{t}Bu). ^{13}C{^{1}H} NMR: δ 253.7 (d, J_{CP} = 30, MoCO), 246.9 (d, J_{CP} = 3, MoCO), 156.6 [d, J_{CP} = 24, $C^2(C_6H_2)$], 153.9 [s, $C^4(C_6H_2)$], 152.3 [d, J_{CP} = 3, $C^2(C_6H_2)$], 130.0 [d, J_{CP} = 58, $C^1(C_6H_2)$], 123.8 [d, J_{CP} = 10, $C^3(C_6H_2)$], 123.7 [d, J_{CP} = 18, $C^3(C_6H_2)$], 95.5 (s, Cp), 52.9 (d, J_{CP} = 5, OMe), 39.7, 35.1, 30.0 [3s, $C^1(^t$Bu)], 33.9, 32.6, 30.9 [3s, C^2(tBu)].

Preparation of [MoCp{*S*,*P*-(MeS)P(O)R*}(CO)$_2$] (5). Methyl iodide (27 μL, 0.43 mmol) was added to a dichloromethane solution (10 mL) of compound **3** (0.030 g, 0.043 mmol) at 290 K, and the mixture was stirred for 15 min to give a yellow solution. Solvent was then removed under vacuum and the residue was chromatographed on alumina at 253 K. Elution with tetrahydrofuran/petroleum ether (1/3) gave a yellow fraction which yielded, after removal of solvents, compound **5** as a yellow microcrystalline solid (0.022 g, 92%). Anal. Calcd for $C_{26}H_{37}MoPO_3S$: C, 56.11; H, 6.70. Found: C, 55.65; H, 6.56. ^{1}H NMR: δ 7.33 (dd, J_{HP} = 6, J_{HH} = 2, 1H, C_6H_2), 7.20 (t, J_{HP} = J_{HH} = 2, 1H, C_6H_2), 4.59 (s, 5H, Cp), 2.09 (d, J_{HP} = 3, 3H, SMe), 1.67, 1.46, 1.30 (3s, 3 x 9H, ^{t}Bu). ^{13}C{^{1}H} NMR: δ 242.1 (d, J_{CP} = 40, MoCO), 239.7 (s, MoCO), 157.0 [d, J_{CP} = 26, $C^2(C_6H_2)$], 152.3 [s, $C^4(C_6H_2)$], 151.0 [s, $C^2(C_6H_2)$], 143.0 [d, J_{CP} = 28, $C^1(C_6H_2)$], 122.5 [d, J_{CP} = 8, $C^3(C_6H_2)$], 122.3 [d, J_{CP} = 15, $C^3(C_6H_2)$], 93.7 (s, Cp), 41.6, 39.9, 35.0 [3s, $C^1(^t$Bu)], 34.2, 33.4, 30.9 [3s, $C^2(^t$Bu)], 19.0 (s, SMe).

Preparation of [MoCp{*S*,*P*-SP(OMe)R*}(CO)$_2$] (6). Solid $(Me_3O)BF_4$ (0.010 g, 0.067 mmol) was added to a dichloromethane solution (10 mL) of compound **3** (0.040 g, 0.058 mmol) at 273 K, and the mixture was stirred for 2 min to give an orange-yellow solution. Solvent was then removed under vacuum and the residue was chromatographed on alumina at 253 K. Elution with dichloromethane/petroleum ether (1/9) gave a yellow fraction which yielded, after removal of solvents, compound **6** as an orange microcrystalline solid (0.016 g, 50%). Elution with tetrahydrofuran/petroleum ether (1/3) gave a yellow fraction which yielded analogously compound **5** as a yellow microcrystalline solid (0.014 g, 43%). Anal. Calcd for $C_{26}H_{37}MoPO_3S$: C, 56.12; H, 6.70. Found: C, 56.58; H, 6.55. ^{1}H NMR: δ 7.37 (dd, J_{HP} = 6, J_{HH} = 2, 1H, C_6H_2), 7.26 (t, J_{HP} = J_{HH} = 2, 1H, C_6H_2), 4.91 (s, 5H, Cp), 3.18 (d, J_{HP} = 16, 3H, OMe), 1.62, 1.57, 1.30 (3s, 3 x 9H, ^{t}Bu). ^{13}C{^{1}H} NMR: δ 251.1 (d, J_{CP} = 27, MoCO), 239.4 (s, MoCO), 156.4 [d, J_{CP} = 24, $C^2(C_6H_2)$], 156.7 [s, $C^4(C_6H_2)$], 152.1 [d, J_{CP} = 4, $C^2(C_6H_2)$], 131.8 [d, J_{CP} = 66, $C^1(C_6H_2)$], 123.3 [d, J_{CP} = 11, $C^3(C_6H_2)$], 122.5 [d, J_{CP} = 18, $C^3(C_6H_2)$], 94.4 (s, Cp), 52.7 [d, J_{CP} = 7, OMe], 41.1, 40.3 [2d, J_{CP} = 4, $C^1(^t$Bu)], 34.9 [s, $C^1(^t$Bu)], 33.8, 35.3, 30.9 [3s, $C^2(^t$Bu)].

Preparation of [MoCp{*S*,*P*-SP(OC(O)C$_2$H$_3$)R*}(CO)$_2$] (7). Neat acryloyl chloride (10 μL, 0.121 mmol) was added to a dichloromethane solution (10 mL) of compound **3** (0.036 g, 0.052 mmol) at room temperature, and the mixture was stirred for 10 min to give an orange solution. Solvent was then removed under vacuum, and the residue was chromatographed on alumina at 285 K. Elution with dichloromethane/petroleum ether (1/3) gave an orange fraction yielding, after removal of solvents, compound **7** as an orange solid (0.026 g, 84%). The crystals used in the X-ray study were grown from a concentrated petroleum ether solution of the complex at 253 K. Anal. Calcd for $C_{28}H_{37}MoO_4PS$: C, 56.37; H, 6.25. Found: C, 56.33; H, 6.34. ^{1}H NMR: δ 7.38 (dd, J_{HP} = 7, J_{HH} = 2, 1H, C_6H_2), 7.29 (t, J_{HP} = J_{HH} = 2, 1H, C_6H_2), 6.42 (dd, J_{HH} = 17, J_{HP} = 1, 1H, trans-CH_2), 6.07 (ddd, J_{HH} = 17, J_{HH} = 10, J_{HP}= 1, 1H, CH), 5.91 (d, J_{HH} = 10, 1H, cis-CH_2), 4.93 (s, 5H, Cp), 1.63 (s, 18H, ^{t}Bu), 1.31 (s, 9H, ^{t}Bu). ^{13}C{^{1}H} NMR: δ 251.0 (d, J_{CP} = 28, MoCO), 237.1 (s, MoCO), 160.1 [d, J_{CP} = 10, $C(O)C_2H_3$], 158.5 [d, J_{CP} = 27, $C^2(C_6H_2)$], 152.7 [d, J_{CP} = 5, $C^2(C_6H_2)$], 156.7 [s, $C^4(C_6H_2)$], 133.2 [d, J_{CP} = 59, $C^1(C_6H_2)$], 132.8 (s, CH_2), 129.3 (s, CH), 123.7 [d, J_{CP} = 11, $C^3(C_6H_2)$], 123.0 [d, J_{CP} = 18, $C^3(C_6H_2)$], 94.5 (s, Cp), 41.2

[J_{CP} = 3, C^1(*t*Bu)], 40.5 [J_{CP} = 5, C^1(*t*Bu)], 35.1 [s, C^1(*t*Bu)], 33.9, 33.6, 30.9 [3s, C^2(*t*Bu)].

Preparation of [MoCp{*S*,*P*-SP(OH)R*}(CO)$_2$] (8). Solid $(NH_4)PF_6$ (0.017 g, 0.104 mmol) was added to a tetrahydrofuran solution (10 mL) of compound **3** (0.036 g, 0.052 mmol) at room temperature, and the mixture was stirred for 10 min to give an orange solution. After removal of solvent under vacuum, the residue was extracted with petroleum ether and the extract filtered. Removal of solvent from the filtrate yielded compound **8** as an orange, very air-sensitive solid (0.020 g, 71%). ^{1}H NMR (200.13 MHz): δ 7.33 (dd, J_{HP} = 6, J_{HH} = 2, 1H, C_6H_2), 7.22 (t, J_{HP} = J_{HH} = 2, 1H, C_6H_2), 6.82 (br, 1H, OH), 4.91 (s, 5H, Cp), 1.65, 1.62, 1.29 (3s, 3 x 9H, *t*Bu). ^{13}C{^{1}H} NMR (243 K): δ 251.7 (d, J_{CP} = 28, MoCO), 241.1 (s, MoCO), 157.8 [d, J_{CP} = 24, $C^2(C_6H_2)$], 151.5 [d, J_{CP} = 4, $C^2(C_6H_2)$], 156.3 [s, $C^4(C_6H_2)$], 133.1 [d, J_{CP} = 62, $C^1(C_6H_2)$], 122.9 [d, J_{CP} = 11, $C^3(C_6H_2)$], 122.2 [d, J_{CP} = 17, $C^3(C_6H_2)$], 94.5 (s, Cp), 41.1 [d, J_{CP} = 4, C^1(*t*Bu)], 40.1 [d, J_{CP} = 5, C^1(*t*Bu)], 34.9 [s, C^1(*t*Bu)], 33.9, 33.5, 30.9 [3s, C^2(*t*Bu)].

Preparation of [MoCp{*S*,*P*-SP(OSiMe$_3$)R*}(CO)$_2$] (9). Neat $SiMe_3Cl$ (0.014 μL, 0.108 mmol) was added to a dichloromethane solution (10 mL) of compound **3** (0.036 g, 0.052 mmol) at room temperature, and the mixture was stirred for 10 min to give an orange solution. After removal of solvent under vacuum, the residue was extracted with petroleum ether and the extracts were filtered. Removal of solvent from the filtrate yielded compound **9** as an orange solid (0.029 g, 91%). The crystals used in the X-ray study were grown from a concentrated petroleum ether solution of the complex at 253 K. Anal. Calcd for $C_{28}H_{43}MoO_3PSSi$: C, 54.71; H, 7.05. Found: C, 54.62; H, 7.14. ^{1}H NMR (200 MHz): δ 7.31 (dd, J_{HP} = 6, J_{HH} = 2, 1H, C_6H_2), 7.20 (t, J_{HP} = J_{HH} = 2, 1H, C_6H_2), 4.83 (s, 5H, Cp), 1.64, 1.61, 1.29 (3s, 3 x 9H, *t*Bu), 0.21 (s, 9H, SiMe). ^{13}C{^{1}H} NMR: δ 252.6 (d, J_{CP} = 29, MoCO), 240.7 (s, MoCO), 157.5 [d, J_{CP} = 26, $C^2(C_6H_2)$], 151.2 [d, J_{CP} = 4, $C^2(C_6H_2)$], 155.0 [s, $C^4(C_6H_2)$], 137.7 [d, J_{CP} = 60, $C^1(C_6H_2)$], 122.8 [d, J_{CP} = 11, $C^3(C_6H_2)$], 122.2 [d, J_{CP} = 17, $C^3(C_6H_2)$], 94.4 (s, Cp), 41.2 [d, J_{CP} = 3, C^1(*t*Bu)], 40.3 [d, J_{CP} = 4, C^1(*t*Bu)], 35.0 [s, C^1(*t*Bu)], 34.2, 33.7, 30.9 [3s, C^2(*t*Bu)], 1.0 (s, SiMe).

Preparation of [MoCp{*S*,*P*-SP(OSnMe$_3$)R*}(CO)$_2$] (10). The procedure is analogous to that described for **9**, but using solid $SnMe_3Cl$ (0.031 g, 0.156 mmol) instead. After similar workup, compound **10** was isolated as an orange solid (0.032 g, 87%). Anal. Calcd for $C_{28}H_{43}MoO_3PSSn$: C, 47.68; H, 6.14. Found: C, 47.44; H, 6.19. ^{1}H NMR (200 MHz): δ 7.28 (dd, J_{HP} = 5, J_{HH} = 2, 1H, C_6H_2), 7.16 (t, J_{HP} = J_{HH} = 2, 1H, C_6H_2), 4.78 (s, 5H, Cp), 1.64, 1.61, 1.29 (3s, 3 x 9H, *t*Bu), 0.57 (s, 9H, SnMe). ^{13}C{^{1}H} NMR: δ 253.0 (d, J_{CP} = 28, MoCO), 243.4 (s, MoCO), 156.8 [d, J_{CP} = 23, $C^2(C_6H_2)$], 154.1 [s, $C^4(C_6H_2)$], 150.2 [s, $C^2(C_6H_2)$], 139.8 [d, J_{CP} = 57, $C^1(C_6H_2)$], 122.3 [d, J_{CP} = 11, $C^3(C_6H_2)$], 121.3 [d, J_{CP} = 16, $C^3(C_6H_2)$], 94.1 (s, Cp), 41.2 [d, J_{CP} = 2, C^1(*t*Bu)], 40.1 [d, J_{CP} = 5, C^1(*t*Bu)], 34.9 [s, C^1(*t*Bu)], 34.2, 33.6, 31.0 [3s, C^1(*t*Bu)], –1.2 (s, SnMe).

Preparation of [MoCp{*S*,*P*-SP(OZrCp$_2$Cl)R*}(CO)$_2$] (11). The procedure is analogous to that described for **9**, but using solid $[ZrCp_2Cl_2]$ (0.015 g, 0.052 mmol) instead. After similar workup, compound **11** was isolated as an orange solid (0.034 g, 82%). Anal. Calcd for $C_{35}H_{44}ClMoO_3PSZr$: C, 52.65; H, 5.55. Found: C, 52.24; H, 5.39. ^{1}H NMR (200 MHz): δ 7.30 (dd, J_{HP} = 6, J_{HH} = 2, 1H, C_6H_2), 7.19 (t, J_{HP} = J_{HH} = 2, 1H, C_6H_2), 6.54, 6.49, 4.83 (3s, 3 x 5H, Cp), 1.73, 1.62, 1.30 (3s, 3 x 9H, *t*Bu).

Table 6: Crystal Data for New Compounds.

	7	**9**
mol formula	$C_{28}H_{37}MoO_4PS$	$C_{28}H_{43}MoO_3PSSi$
mol wt	596.55	614.69
cryst syst	triclinic	monoclinic
space group	*P*–1	$P2_1/c$
radiation (λ, Å)	0.71073	1.54184
a, Å	10.891(2)	14.9470(3)
b, Å	10.945(2)	10.0787(2)
c, Å	13.589(3)	21.2080(4)
α, deg	90.011(3)	90
β, deg	100.921(3)	106.4360(10)
γ, deg	114.499(3)	90
V, Å^3	1441.7(5)	3064.35(10)
Z	2	4
calcd density, g cm^{-3}	1.374	1.332
absorp coeff, mm^{-1}	0.613	5.205
temperature, K	120(2)	150(2)
θ range (deg)	2.05 to 27.15	3.08 to 68.21
index ranges (*h*, *k*, *l*)	–17, 13; –14, 14; 0, 17	–17, 17; 0, 12; 0, 25
no. of reflns collected	17186	19119
no. of indep reflns (R_{int})	6327 (0.0267)	5568 (0.0476)
reflns with $I > 2\sigma(I)$	5731	4899
R indexes [data with $I > 2\sigma(I)$][a]	R_1 = 0.0228 wR_2 = 0.060[b]	R_1 = 0.0537 wR_2 = 0.1473[c]
R indexes (all data)[a]	R_1 = 0.0267 wR_2 = 0.0615[b]	R_1 = 0.0616 wR_2 = 0.1575[c]
GOF	1.07	1.079
no. of restraints/params	0 / 329	0 / 328
$\Delta\rho$(max., min.), eÅ^{-3}	0.47, –0.402	1.398, –0.787

[a] $R = \Sigma||F_o| - |F_c|| / \Sigma|F_o|$. $wR = [\Sigma w(|F_o|^2 - |F_c|^2)^2 / \Sigma w|F_o|^2]^{1/2}$. $w = 1/[\sigma^2(F_o^2) + (aP)^2 + bP]$ where $P = (F_o^2 + 2F_c^2)/3$. [b] a = 0.0313, b = 0.4264. [c] a = 0.0000, b = 34.3529.

X-Ray Crystal Structure Determination for Compound 7

Data collection was performed on a Smart-CCD-1000 BRUKER diffractometer using graphite-monochromated Mo-Kα radiation at 120 K. Cell dimensions and orientation matrixes were initially determined from least-squares refinements on reflections measured in 3 sets of 30 exposures collected in 3 different ω regions and eventually refined against all reflections. The software SMART[26] was used for collecting frames of data, indexing reflections, and determining lattice parameters. The collected frames were then processed for integration by the software SAINT,[26] and a multi-scan absorption correction was applied with SADABS.[27] Using the program suite WinGX,[28] the structure was solved by Patterson interpretation and phase expansion using SHELXL97,[29] and refined

with full-matrix least squares on F^2 using SHELXL97. All non-hydrogen atoms were refined anisotropically. All hydrogen atoms were fixed at calculated geometric positions except for H(4), which was located in the Fourier map and refined. All hydrogen atoms were given an overall isotropic thermal parameter. Crystallographic data and structure refinement details are collected in Table 6.

X-Ray Crystal Structure Determination for Compound 9

Data collection was performed at 150 K on a Nonius KappaCCD single crystal diffractometer, using Cu-Kα radiation. Images were collected at a 29 mm fixed crystal-detector distance, using the oscillation method, with 1.5º oscillation and 60 s exposure time per image. Data collection strategy was calculated with the program Collect.[30] Data reduction and cell refinement were performed with the programs HKL Denzo and Scalepack.[31] A semi-empirical absorption correction was applied using the program SORTAV.[32] Structure solution and refinements were performed as described for **7**. All non-hydrogen atoms were refined anisotropically, and all hydrogen atoms were fixed at calculated geometric positions and were given an overall isotropic thermal parameter. Crystallographic data and structure refinement details are collected in Table 6.

Computational Details

All DFT calculations were carried out using the GAUSSIAN03 package,[33] in which the hybrid method B3LYP was used with the Becke three-parameter exchange functional,[34] and the Lee-Yang-Parr correlation functional.[35] An accurate numerical integration grid (99,590) was used for all the calculations via the keyword Int=Ultrafine. Effective core potentials and their associated double-ζ LANL2DZ basis set were used for the metal atoms.[36] The light elements (P, O, S, C and H) were described with the 6-31G* basis.[37] Geometry optimizations were performed under no symmetry restrictions, using initial coordinates derived from X-ray data of compounds **5** and **6**, and frequency analysis were performed to ensure that minimum structures with no imaginary frequencies were achieved. Molecular orbitals and vibrational modes were visualized using the MOLEKEL program.[38] The topological analysis of the electron density was carried out with the Xaim routine.[39]

Notes and references

[a]*Departamento de Química Orgánica e Inorgánica / IUQOEM, Universidad de Oviedo, E-33071 Oviedo, Spain. E-mail: garciavdaniel@uniovi.es (D.G-V.), mara@uniovi.es (M.A.R.)*

†Electronic supplementary information (ESI) available: A PDF file containing the complete reference 33 and details of DFT calculations (drawings, atomic coordinates and energies of compounds **2**, **3**, **5**, **6**, and **8**). CCDC-995392 (**7**) and 995393 (**9**). DOI: 10.1039/b000000x/

1 L. D. Quin, *Coord. Chem. Rev.* 1994, **137**, 525.

2 L. N. Heydorn, P. C. Burgers, P. J. A. Ruttink and J. K. Terlouw, *Chem. Phys. Lett.* 2003, **368**, 584, and references therein.

3 R. Menye-Biyogo, F. Delpech, A. Castel, H. Gornitzka and P. Rivière, *Angew. Chem. Int. Ed.* 2003, **42**, 5610.

4 M. Alonso, M. A. Alvarez, M. E. García, M. A. Ruiz, H. Hamidov and J. C. Jeffery, *J. Am. Chem. Soc.* 2005, **127**, 15012.

5 M. Alonso, M. A. Alvarez, M. E. García, D. García-Vivó and M. A. Ruiz, *Inorg. Chem.* 2010, **49**, 8962.

6 P. S. Braterman, *Metal Carbonyl Spectra*, Academic Press, London, U. K., 1975.

7 C. J. Jameson, in *Phosphorus-31 NMR Spectroscopy in Stereochemical Analysis*, J. G. Verkade and L. D. Quin, Eds., VCH, Deerfield Beach, FL, 1987, Chapter 6.

8 A general trend established for $^2J_{XY}$ in complexes of the type $[MCpXYL_2]$ is that $|J_{cis}| > |J_{trans}|$. See, for instance, the reference 7 and also: B. Wrackmeyer, H. G. Alt and H. E. Maisel, *J. Organomet. Chem.* 1990, **399**, 125.

9 (a) W. Koch and M. C. Holthausen, *A Chemist's Guide to Density Functional Theory, 2nd ed.*, Wiley-VCH, Weinheim, Germany, 2002. (b) T. Ziegler, *Chem. Rev.* 1991, **91**, 651. (c) J. B. Foresman and Æ. Frisch, *Exploring Chemistry with Electronic Structure Methods, 2nd ed.*, Gaussian, Inc., Pittsburg, 1996.

10 (a) R. F. W. Bader, *Atoms in Molecules – A Quantum Theory*, Oxford University Press, Oxford, 1990. (b) R. F. W. Bader, *Chem. Rev.* 1991, **91**, 893.

11 P. Macchi and A. Sironi, *Coord. Chem. Rev.* 2003, **238-239**, 383.

12 R. S. Mulliken, *J. Chem. Phys.* 1955, **23**, 1833.

13 Mulliken population analysis fails to give a useful and reliable characterization of the charge distribution in many cases, especially when highly ionic compounds and diffuse basis functions are involved. Charges calculated according to the natural population analysis (NPA) do not show these deficiencies and are more independent of the basis set: (a) A. E. Reed, R. B. Weinstock and F. J. Weinhold, *Chem. Phys*. 1985, **83**, 735. (b) A. E. Reed, L. A. Curtis and F. Weinhold, *Chem. Rev.* 1988, **88**, 899.

14 B. Cordero, V. Gómez, A. E. Platero-Prats, M. Revés, J. Echeverría, E. Cremades, F. Barragán and S. Alvarez, *Dalton Trans.* 2008, 2832.

15 B. Alvarez, M. A. Alvarez, I. Amor, M. E. García, D. García-Vivó, M. A. Ruiz and J. Suárez, *Inorg. Chem.* 2012, **51**, 7810.

16 W. Malisch, K. Grün, U.-A. Hirth and M. Noltemeyer, *J. Organomet. Chem.* 1996, **513**, 31.

17 H.-U. Reisacher, W. F. McNamara, E. N. Duesler and R. T. Paine, *Organometallics* 1997, **16**, 449.

18 H. Alper, F. W. B. Einstein, F. W. Harstock and R. H. Jones, *Organometallics* 1987, **6**, 829.

19 C. J. Cramer, *Essentials of Computational Chemistry, 2nd ed.*, Wiley, Chichester, U.K., 2004.

20 J. E. Huheey, E. A. Keiter and R. L. Keiter, *Inorganic Chemistry: Principles of Structure and Reactivity, 4th ed.*, HarperCollins College Publishers, New York, USA, 1993, p. A-25.

21 M. Alonso, M. A. Alvarez, M. E. García, M. A. Ruiz, H. Hamidov and J. C. Jeffery, *Inorg. Chem.* 2010, **49**, 11595.

22 T. Gebauer, G. Frenzen and K. Dehnicke, *Z. Naturforsh B* 1993, **48**, 1661.

23 H. Wilkens, A. Ostrowski, J. Jeske, F. Ruthe, P. G. Jones and R. Streubel, *Organometallics* 1999, **18**, 5627.

24 W. L. F. Armarego and C. Chai, *Purification of Laboratory Chemicals, 5th Ed.*, Butterworth-Heinemann, Oxford, U. K., 2003.

25 W. Adam, J. Bialas and L. Hadjiarapoglou, *Chem. Ber.* 1991, **124**, 2377.

26 *SMART & SAINT Software Reference Manuals, version 5.051* (Windows NT version), Bruker Analytical X-ray Instruments, Madison, WI, 1998.

27 G. M. Sheldrick, *SADABS, Program for Empirical Absorption Correction*, University of Göttingen, Göttingen, Germany, 1996.
28 L. J. Farrugia, *J. Appl. Crystallogr.* 1999, **32**, 837.
29 G. M. Sheldrick, *Acta Crystallogr. Sect. A* 2008, **64**, 112.
30 *Collect*, Nonius BV, Delft, The Netherlands, 1997-2004.
31 Z. Otwinowski and W. Minor, *Methods Enzymol.* 1997, **276**, 307.
32 R. H. Blessing, *Acta Crystallogr., Sect A* 1995, **51**, 33.
33 M. J. Frisch, et al., *Gaussian 03, Revision B.02*, Gaussian, Inc., Wallingford CT, 2004.
34 A. D. Becke, *J. Chem. Phys.* 1993, **98**, 5648.
35 C. Lee, W. Yang and R. G. Parr, *Phys. Rev. B* 1988, **37**, 785.
36 P. J. Hay and W. R. Wadt, *J. Chem. Phys.* 1985, **82**, 299.
37 (a) P. C. Hariharan and J. A. Pople, *Theor. Chim. Acta* 1973, **28**, 213. (b) G. A. Petersson and M. A. Al-Laham, *J. Chem. Phys.* 1991, **94**, 6081. (c) G. A. Petersson, A. Bennett, T. G. Tensfeldt, M. A. Al-Laham, W. A. Shirley and J. Mantzaris, *J. Chem. Phys.* 1988, **89**, 2193.
38 S. Portmann and H. P. Lüthi, *MOLEKEL, An Interactive Molecular Graphics Tool*, CHIMIA 2000, **54**, 766.
39 J. C. Ortiz and C. Bo, *Xaim*, Departamento de Química Física e Inorgánica, Universidad Rovira i Virgili, Tarragona, Spain, 1998.